Vascular Hypertrophy in Experimental Diabetes
Role of Advanced Glycation End Products

Jonathan R. Rumble, Mark E. Cooper, Tina Soulis, Alison Cox, Leonard Wu, Sherif Youssef, Mariusz Jasik, George Jerums, and Richard E. Gilbert

Department of Medicine, University of Melbourne, Austin and Repatriation Medical Center, Heidelberg, Victoria 3084, Australia

Abstract

The accelerated formation of advanced glycation end products (AGEs) and the overexpression of transforming growth factor beta (TGF-β) have both been implicated in the pathogenesis of diabetic microvascular and macrovascular complications. Previous studies in our laboratory have demonstrated that the vascular changes in diabetes include hypertrophy of the mesenteric vasculature. To examine the role of AGEs in this process, streptozotocin-induced diabetic rats and control animals were randomized to receive aminoguanidine, an inhibitor of AGE formation, or no treatment. Animals were studied at 7 d, 3 wk, and 8 mo after induction of diabetes. When compared with control animals, diabetes was associated with an increase in mesenteric vascular weight and an increase in media wall/lumen area. By Northern analysis, TGF-β1 gene expression was increased 100–150% ($P < 0.01$) and α1 (IV) collagen gene expression was similarly elevated to 30–110% compared to controls ($P < 0.05$). AGEs and extracellular matrix were present in abundance in diabetic but not in control vessels. Treatment of diabetic rats with aminoguanidine resulted in significant amelioration of the described pathological changes including overexpression of TGF-β1 and α1 (IV) collagen. These data implicate the formation of AGEs in TGF-β overexpression and tissue changes which accompany the diabetic state. (*J. Clin. Invest.* 1997. 99:1016–1027.) Key words: mesenteric arteries • transforming growth factor beta • glycosylation end products, advanced • diabetes mellitus, experimental

Introduction

Extracellular matrix (ECM)[1] expansion and vascular hypertrophy have been implicated in the pathogenesis of the microvascular complications of diabetes (1). The formation of long lived nonenzymatically glycated proteins has been postulated as a fundamental mechanism in the pathogenesis of these complications (2). Aminoguanidine (AG), a hydrazine-like compound which inhibits the formation of advanced glycation end-products (AGEs), has been shown to retard the development of nephropathy and retinopathy in experimental animals (3, 4).

Studies in our laboratory have shown that the mesenteric vascular tree, a site of intensive study in other vascular disease states, such as hypertension (5) and atherosclerosis (6), exhibits vascular hypertrophy after 3 wk of experimental diabetes (7–9). In these vessels there is evidence of ECM expansion, intimal proliferation, and medial enlargement (8).

Transforming growth factor-beta (TGF-β) has been implicated in the vascular remodeling that accompanies hypertension (10) and in the pathogenesis of diabetic nephropathy (11). The actions of this multifunctional cytokine include the promotion of smooth muscle cell growth (12), intimal hyperplasia (13), and ECM expansion (14). Both in vitro (15) and in vivo (16) studies have shown the ability of AGEs to increase TGF-β production.

The present study examines the role of AGEs and TGF-β1 expression in diabetes-related mesenteric vascular growth. Vascular changes at this site may reflect those found in other areas of vascular injury, such as the glomerulus, which like the mesenteric vasculature is subject to hyperperfusion in diabetes (17).

Methods

Animals. Male Sprague Dawley rats aged 8 wk, weighing between 200 and 250 g were randomized to receive streptozotocin (STZ) at a dose of 45 mg/kg (diabetic) or citrate buffer alone (control). The animals were then further randomized to receive either no treatment or aminoguanidine (Regis Technologies, Inc., Morton Grove, IL) in drinking water (diabetic dose = 1 g/liter, control = 3 g/liter), yielding four treatment groups: control, control with AG treatment, diabetes, diabetes with AG treatment. All rats were given free access to standard chow containing 20% protein (Clark, King & Co, Melbourne, Australia). Only STZ-treated animals with plasma glucose levels > 15 mmol/liter were considered diabetic and included in the study. Animals were killed at 7 d, 3 wk, and 8 mo. Diabetic rats killed at 1 and 3 wk after STZ injection did not receive insulin. However, diabetic animals, untreated or treated with AG, studied for 8 mo, received 6 U insulin zinc suspension (Ultratard HM; Novo Nordisk, Bagsvaerd, Denmark) injected subcutaneously three times per week to maintain body weight and improve long-term survival.

Immediately before being killed, rats were weighed and systolic blood pressure was determined by tail cuff plethysmography (18). Animals were killed by decapitation and blood collected for determination of plasma glucose by glucose oxidase technique (19) and glycated hemoglobin (HbA_{1c}) by HPLC (Bio-Rad, Richmond, CA; 20). To exclude the possibility of long-term toxicity of AG, liver and renal function tests, electrolytes, and hemoglobin were measured in control and diabetic rats (with and without AG treatment) at week 32. The mesenteric vessels were then removed and stripped of surrounding fat, connective tissue and veins to yield the superior mesenteric arterial tree as previously described (8). The vessels were weighed, snap frozen in liquid nitrogen, and subsequently stored at −80°C.

Northern analysis. Mesenteric arteries stored at −80°C were homogenized (Ultra-Turrax; Janke and Kunkel, Staufen, Germany) and total RNA was isolated by the acid guanidinium thiocyanate-phenol-chloroform extraction method (21). RNA purity and concentration were determined spectrophotometrically. 20-μg samples were denatured and electrophoresed through 0.8% agarose formaldehyde gels. RNA integrity was verified by examination of the 28S and 18S ribosomal RNA bands of ethidium bromide-stained material under ultraviolet light. RNA was then transferred onto nylon filters (Hybond-N; Amersham International, Little Chalfont, UK) by capillary action and fixed by ultraviolet irradiation.

Filters were hybridized with a 985-bp cDNA probe coding for rat TGF-β1 (gift of Dr. S.W. Qian, National Institutes of Health, Bethesda, MD) and a 1.8-kb cDNA probe coding for mouse α1 (IV) collagen (gift of Dr. R. Timpl, Max Plank Institute, Martinsried, Germany). To assess the biological activity of TGF-β1, Northern analysis of the TGF-β induced gene, βig-h3 (TGF-β–inducible gene *h3*) (22) was also performed. A 2.7-kb cDNA probe coding for human βig-h3 (gift of Dr. K. Bennett, Bristol Myers Squibb, Seattle, WA) was used. Probes were labeled with [α-^{32}P]dCTP (DuPont-NEN, Boston, MA) by random primed DNA synthesis (Boehringer Mannheim GmBH, Mannheim, Germany). For TGF-β1, hybridization was performed at 65°C for 16–20 h in a solution containing 1% BSA, 7% SDS, 0.5 M NaHPO$_4$, and 1 mM EDTA followed by washing three times at 65°C for 15 min in 1% SDS, 40 mM NaHPO$_4$, and 1 mM EDTA. Hybridization of filters for α1 (IV) collagen and βig-h3 were performed at 42°C for 24 h in 50% formamide, 45 mM Na$_2$HPO$_4$, 5× Denhardt's solution, 0.5% SDS, and sonicated salmon sperm DNA. Filters were then washed in solutions of decreasing ionic strength and increasing temperature. The final stringency was 0.1× standard saline citrate (SSC) with 0.1% SDS for 20 min at 42°C. Intensity of hybridization was quantified using a phosphorescent imager (model Fujix BASS 3000; Fuji Photo Film Co., Tokyo, Japan). All results were corrected for differences in RNA loading and transfer by rehybridization with an oligonucleotide probe for 18S rRNA end-labeled with [α-^{32}P]dCTP by terminal transferase (Boehringer Mannheim). Results were expressed as the ratio of image intensity of TGF-β1, α1 (IV) collagen, or βig-h3 to 18S relative to control vessels which were arbitrarily assigned a value of 1.

In situ hybridization. In situ hybridization studies of mesenteric arteries were performed in a subset of animals studied at 7 d duration of diabetes and compared with their nondiabetic counterparts. This time was chosen on the basis of pilot studies of gene expression assessed by Northern analysis which indicated an early increase in TGF-β1 mRNA.

The cDNAs coding for TGF-β1 and βig-h3 were cloned into pBluescript KS+ and SK+, respectively (Stratagene Inc., La Jolla, CA). The TGF-β1 cDNA was linearized with XbaI, and βig-h3 was linearized with HindIII. Antisense riboprobes were produced using T3 RNA polymerase. The cDNA probe for α1 (IV) collagen was cloned into pGEM 3Z (Promega Corp., Madison, WI) and linearized with BamHI to produce an antisense riboprobe with SP6 RNA polymerase. 500 ng of linearized template was added to a reaction mixture of transcription buffer (final volume 20 μl) containing 6 mM dithiothreitol, 333 μM ATP, CTP, GTP, 12 μM UTP, 100 μCi [^{33}P]UTP (3,000 Ci/mmol; DuPont-NEN), 20 U RNAsin (Boehringer Mannheim) and 20 U RNA polymerase (Boehringer Mannheim). The reaction mixture was incubated at 37°C for 90 min after which the DNA template was digested with 1 U ribonuclease (RNase) free DNAse for 15 min. The riboprobe was precipitated by ammonium acetate and ethanol using yeast tRNA as a carrier and then reconstituted in 100 μl of DEPC treated water. Purified riboprobe length was adjusted to ∼ 150 bases by alkaline hydrolysis (23).

5-μm thick sections were cut from formalin-fixed paraffin-embedded mesenteric vessels, placed onto slides precoated with 3-aminopropyltriethoxysilane and baked overnight at 37°C. In situ hybridization was performed as previously described (24). In brief, tissue sections were dewaxed and rehydrated in graded ethanol and milliQ

water, equilibrated in P buffer (50 mM Tris-HCl, pH 7.5, 5 mM EDTA) and incubated in 125 μg/ml Pronase E in P buffer for 10 min at 37°C. Sections were then washed in 0.1 M sodium phosphate buffer (pH 7.2), briefly refixed in 4% paraformaldehyde for 10 min, rinsed in milliQ water, dehydrated in 70% ethanol, and air dried. Hybridization buffer containing 2 × 10^4 cpm/μl riboprobe in 300 mM NaCl, 10 mM Tris-HCl (pH 7.5), 10 mM Na$_2$HPO$_4$, 5 mM EDTA (pH 8.0), 1 × Denhardt's solution, 50% formamide, 17 mg/ml yeast RNA, 10% wt/vol dextran sulfate was heated to 85°C for 5 min. 25 μl of this solution was then added to each section. Hybridization was performed overnight at 60°C in 50% formamide humidified chambers. Sections hybridized with sense probe for TGF-β1, βig-h3, and α1 (IV) collagen were used as controls for nonspecific binding.

After hybridization, slides were washed in 2× SSC containing 50% formamide prewarmed to 50°C to remove coverslips. Sections were then washed in the above solution for 1 h at 55°C, rinsed three more times in RNase buffer (10 mM Tris–HCl, pH 7.5, 1 mM EDTA, pH 8.0, 0.5 M NaCl) and then incubated with RNase A (150 μg/ml) for 1 h at 37°C. Sections were later washed in 2× SSC for 45 min at 55°C, dehydrated in graded ethanol, air dried, and exposed to x-ray film (BIOMAX MR; Eastman-Kodak, Rochester, NY) for 1–3 d. Slides were then dipped in emulsion (K5; Ilford, Mobberley, UK), stored in a light-free box with desiccant at room temperature for 2 to 3 wk, immersed in developer (D19; Eastman–Kodak), fixed (Hypam; Ilford) and stained with hematoxylin and eosin.

Histology. Histological studies of vascular architecture were performed in a subset of animals studied at 3 weeks. This time was chosen on the basis of previous studies with this model (8). Animals in this subgroup were anesthetized with pentobarbital sodium (Nembutal; Bomac Laboratories, Asquith, Australia) and vessels were perfused at arterial pressure with 2.5% glutaraldehyde via an intraaortic cannula. Tissues were then prepared as previously described (8). In brief, mesenteric vessels were placed in ice-cold phosphate buffer where fat, connective tissue, and veins were removed by blunt dissection. The isolated cleaned mesentery artery and its branches were then examined by dissecting microscope to confirm complete removal of fat before weighing. The resultant vessel preparation was then fixed in 10% formalin and embedded in paraffin. 5-μm thick sections were then obtained for the assessment of vessel media, ECM content, and AGE content. Histological analyses were determined in a median of 18 (range 10–35) vessels per animal.

The proportion of vessel wall occupied by the media was demonstrated immunohistochemically by the presence of α-smooth muscle actin containing cells using the indirect avidin-biotinylated peroxidase method as previously described (25). Sections were incubated with antismooth muscle actin antibody (Biogenes, San Ramon, CA) and immunostaining was quantified using a video-imaging system (model Video Pro 32; Leading Edge, Bedford Park, South Australia, Australia), connected to a light microscope with photographic attachment (model axiophot; Zeiss, Oberkocken, Germany). Using this device, the media (areas stained with the antiactin antibody) and corresponding lumenal areas were expressed as wall/lumen ratio, as previously described in other models of vascular hypertrophy (26, 27).

Vessel type IV collagen content was assessed immunohistochemically using a polyclonal goat anti–bovine/anti–human α1 (IV) collagen antibody (Southern Biotechnology, Birmingham, AL). Tissues were fixed in methyl Carnoy's solution and embedded in paraffin. 4-μm sections were then cut and immunohistochemistry performed using a standard immunohistochemical technique as previously described (28).

AGE staining of tissues was assessed by an immunoperoxidase technique using an anti-AGE antibody. A polyclonal anti-AGE antibody was raised by immunizing New Zealand White Cross rabbits with advanced glycated BSA (AGE-BSA). The latter was prepared by in vitro glycation of crystallized and lyophilized BSA (Fraction V, low endotoxin; Sigma Chemical Co., Clayton, Victoria, Australia) by incubation in the presence of 1 mol/liter glucose in 0.5 mol/liter sodium phosphate buffer containing 1 mmol/liter EDTA, 1 mmol/liter

phenylmethylsulphonyl fluoride, 1 mmol/liter aprotinin, and 1 mmol/liter sodium azide for 120 d (29). The derived solution was then sterilized by passage through a 0.2-μm Millipore membrane and the presence of AGEs confirmed by fluorospectrophotometry (excitation 370 nm, emission 440 nm). Specificity of the antibody for AGE products was confirmed by a competitive RIA using advanced glycated RNase as the radioligand (30). Native (nonglycated) BSA and RNase did not inhibit antibody-tracer binding, while glycated proteins were shown to produce reproducible inhibition curves. The antibody recognizes other glycated species including AGE-keyhole limpet hemocyanin and AGE-collagen, and detects carboxymethyl lysine (CML) complexed collagen and carboxymethyl lysine complexed BSA. This suggests that the antibody recognizes the carboxymethyl lysine epitope of AGEs. This antibody does not detect pentosidine, an AGE that has been detected in vivo (31).

Formalin-fixed paraffin embedded sections (4-μm thick) of the mesenteric vessels were cut, placed on gelatinized slides, rehydrated, and treated with 1% H_2O_2/methanol followed by incubation in Protein Blocking Agent (Lipshaw-Immunon Corp., Pittsburgh, PA) for 20 min at room temperature. Sections were then incubated with anti-AGE antibody for 30 min at room temperature, washed in PBS and incubated with biotinylated swine anti–goat, mouse, rabbit immunoglobulin (Dako Corp., Carpinteria, CA) and peroxidase-conjugated streptavidin (Dako). Peroxidase conjugates were subsequently localized using diaminobenzidine tetrahydrochloride (DAB) as a chromogen. As a control for anti-AGE immunoreactivity, AGEs formed, in vitro, as described above were preincubated with anti-AGE antibody and used in place of the AGE antibody alone in the normal staining procedure. Tissues treated in this manner showed no positive staining.

Quantitation of immunohistochemical staining was performed using a semiquantitative scale, adapted from O'Brien et al. (32), in which two independent observers, blind to the disease status of the animal, graded sections as 0 = absent staining, 1+ = weak staining (< 20% tissue stained), 2+ = moderate staining (20–50% tissue stained) or 3+ = strong staining (> 50% tissue stained).

Staining with Masson's trichrome was performed as originally described (33). 4-μm sections were rehydrated and immersed in potassium dichromate-alcoholic HCl for 30 min, then rinsed in water. Sections were then stained with Celestine Blue-Hematoxylin before rinsing again in water. Sections were subsequently treated with 1% Brilliant Crocein in 1% phosphotungstic acid for 5 min and rinsed in 1% phosphotungstic acid. The final stain was performed by immersing the slides in 0.5% Light Green in 1% acetic acid for 10 min and then washing with 1% aqueous acetic acid. Using this method nuclei are stained black, smooth muscle is stained red, and collagen is stained blue.

AGE radioimmunoassay. To complement the immunohistochemical studies of AGEs, tissue homogenates were obtained from a subset of animals studied at 3 wk and assayed for AGEs by RIA, as previously performed in our laboratory (30). AGE-RNase was iodinated using lactoperoxidase. The AGE-RNase standards (generated as a result of 6 mo incubation of RNase with 0.5 M glucose in 0.2 M phosphate buffer at 37°C) or collagenase extracted mesenteric vessel homogenates were incubated with the antibody and tracer for 5 h at room temperature. Sheep anti–rabbit IgG was then added and incubated overnight at room temperature. Precipitation of proteins was carried out by addition of 8% polyethylene glycol. The minimum concentration detected was 250 ng/ml and the CV of this assay was 11.9%, n = 4, at a concentration of 2,000 ng AGE-RNase/mg protein. The standard curve was generated with serial AGE-RNase dilutions.

Statistics. All data are shown as mean±SE. Data were analyzed by ANOVA using the StatView II program (Abacus Concepts, Inc., Berkeley, CA) on a Macintosh personal computer (Apple Computer, Inc., Cupertino, CA). Comparisons between group means were analyzed by Fisher's least significant difference method (34). Semiquantitative data derived from scoring immunoperoxidase stained sections were analyzed by the Kruskal Wallis test. A *P* value of less than 0.05 was considered statistically significant.

Table I. Clinical Characteristics of Study Rats

Group	n	Body weight	Plasma glucose	Blood pressure
		g	mM	mmHg
A 7 d				
C	9	301±12	7.2±0.3	127±5
D	6	246±18*	24.9±1.6‡	160±8*
DA	6	232±11‡	26.3±1.8‡	126±8§
B 3 wk				
C	12	365±19	6.6±0.2	139±4
D	12	231±12‡	26.1±0.8‡	137±6
DA	9	259±12‡	24.0±1.1‡	146±3
C 8 mo				
C	13	506±11	6.7±0.4	146±3
D	12	352±20‡	26.6±1.8‡	145±5
DA	8	366±42‡	27.5±2.7‡	154±5

Data are shown as mean±SE. *$P < 0.01$, ‡$P < 0.001$ vs. C; §$P < 0.01$ vs. D. C, control; D, diabetic; A, aminoguanidine.

Results

Diabetes was associated with reduced weight gain which was not influenced by AG treatment (Table I). Plasma glucose levels were similar in diabetic animals with and without AG (Table I). Glycated hemoglobin was measured in long-term rats and shown to be increased in diabetic rats (control, 1.7±0.1%; diabetic, 4.6±0.4%; $P < 0.001$) and was not affected by AG treatment (diabetic + AG, 4.4±0.7%; $P < 0.001$ vs. control). Systolic blood pressure was significantly higher in the diabetic group at day seven, compared with controls, and was attenuated by AG treatment (Table I *A*). However, at 3 wk and 8 mo there was no difference in systolic blood pressure among groups (Table I *B* and *C*). Food intake was increased in diabetic animals at 3 wk, compared to controls, but was not influenced by AG treatment (control, 27±2; diabetic, 45±2; diabetic + aminoguanidine, 49±1 g/d; $P < 0.001$ control vs. diabetic).

There was no difference in hemoglobin between control and diabetic rats (control, 15.7±0.4; diabetic, 15.8±0.1 g/dl) and this parameter was not influenced by AG treatment (diabetic + AG, 15.8±0.3 g/dl). There were no significant changes in renal function among the three groups. However, there were significant changes in diabetic rats with respect to liver function tests. Diabetic rats had lower serum albumin, and increased serum alkaline phosphatase (ALP). AG did not influence any parameter except for a modest rise in alanine transaminase (ALT; Table II).

Table II. Biochemical Parameters of Study Rats

Group	Urea	Creatinine	ALP	ALT	Albumin
	(mM)	(μM)	(U/l)	(U/l)	(g/l)
C	7.8±0.1	45±1	170±17	31±4	25.2±1.2
D	7.8±0.9	41±2	605±80*	38±3	21.6±1.4‡
DA	8.7±0.8	43±2	659±101*	56±5*§	20.0±0.8‡

Data are shown at 8 mo as mean±SE. *$P < 0.001$, ‡$P < 0.01$ vs. C; §$P < 0.05$ vs. D. C, control; D, diabetic; A, aminoguanidine.

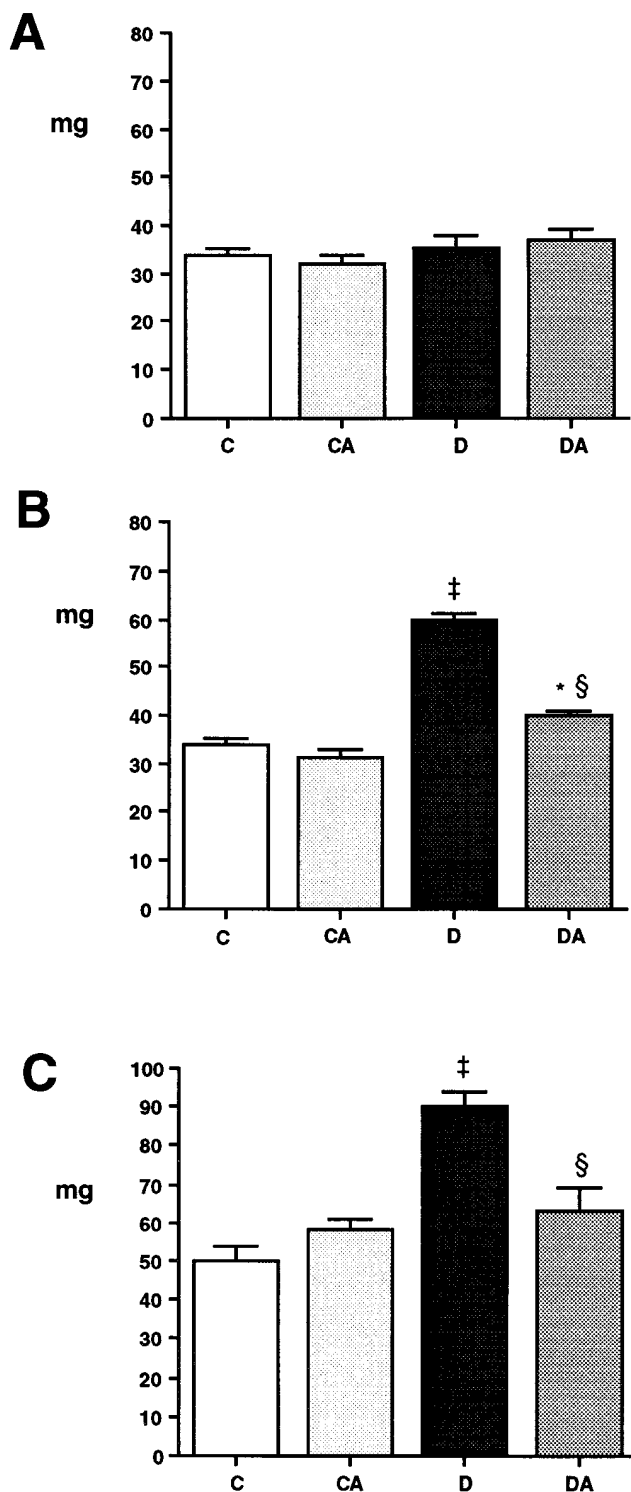Figure 1. Mesenteric vessel weight in mg (mean±SE) at day 7 (A), 3 wk (B), and 8 mo (C). *P < 0.01, ‡P < 0.001 vs. C; §P < 0.001 vs. D. C, control; D, diabetic; A, aminoguanidine.

Figure 2. Mesenteric media wall/lumen area at 3 wk, expressed as mean±SE, relative to control values designated an arbitrary value of 1. *P < 0.001 vs. C; ‡P < 0.001 vs. D. C, control; D, diabetic; A, aminoguanidine.

Mesenteric vessel weight was greater in untreated diabetic rats, compared with control animals, at three wk and 8 mo (Fig. 1, B and C). AG attenuated the increased mesenteric vascular weight in the diabetic animals at both of these time points. Histomorphometric analysis revealed a significant increase in the media wall/lumen area after 3 wk of diabetes
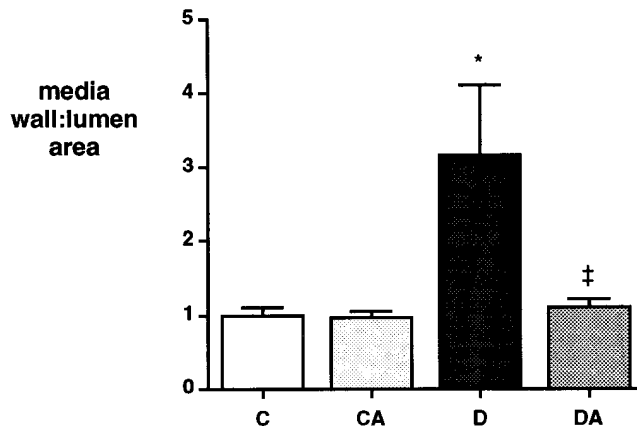
(Fig. 2). Treatment with AG significantly reduced the media wall/lumen area to levels seen in nondiabetic animals. AG treatment did not affect this parameter in nondiabetic animals.

Northern analysis. Mesenteric vessel TGF-β1 mRNA was increased two- to threefold in diabetic animals at all time points compared to their nondiabetic counterparts (Fig. 3 A, Fig. 4). AG prevented this overexpression of TGF-β1 at all time points. Similarly, α1 (IV) collagen gene expression was increased in diabetic animals (Fig. 3 B) and attenuated by AG treatment though not reaching statistical significance at 3 wk (P = 0.09). Gene expression of βig-h3 parallelled changes in gene expression of TGF-β1 and α1 (IV) collagen with increased mRNA in mesenteric vessels from diabetic rats compared with control and AG treated diabetic animals (7 d: control = 1.0±0.1; diabetic = 1.9±0.3; diabetic + AG = 0.6±0.1 arbitrary units; P < 0.001 diabetic vs. other groups). A transient decrease in TGF-β1 expression was noted at day 7 in control animals treated with aminoguanidine when compared with the untreated controls (control, 1.00±0.10; control + aminoguanidine, 0.59±0.04 arbitrary units; P < 0.001). However, at 3 wk and 8 mo there was no difference in TGF-β1 between these groups (3 wk: control, 1.00±0.10; control + aminoguanidine, 0.95±0.18 arbitrary units; 8 mo: control, 1.00±0.11; control + aminoguanidine, 1.07±0.18 arbitrary units).

In situ hybridization. In situ hybridization revealed abundant TGF-β1 gene expression in the adventitia, and to a lesser extent in the intima of mesenteric vessels from diabetic animals (Fig. 5). βig-h3 gene transcript was localized predominantly to the vessel adventitia (Fig. 6) and expression of α1 (IV) collagen mRNA was found in both the media and adventitia of vessels from diabetic animals (Fig. 7). Less intense hybridization for all three transcripts was noted in control and AG treated diabetic animals. No hybridization was observed in sections incubated with sense riboprobes for either TGF-β1, βig-h3, or α1 (IV) collagen.

Type IV collagen staining. Immunohistochemistry demonstrated abundant type IV collagen in the media of mesenteric vessels from diabetic rats. In contrast, only sparse staining was seen in control and AG-treated diabetic animals (Fig. 8).

Trichrome staining. Trichrome stained sections demonstrated expansion of collagenous material in diabetic mesen-
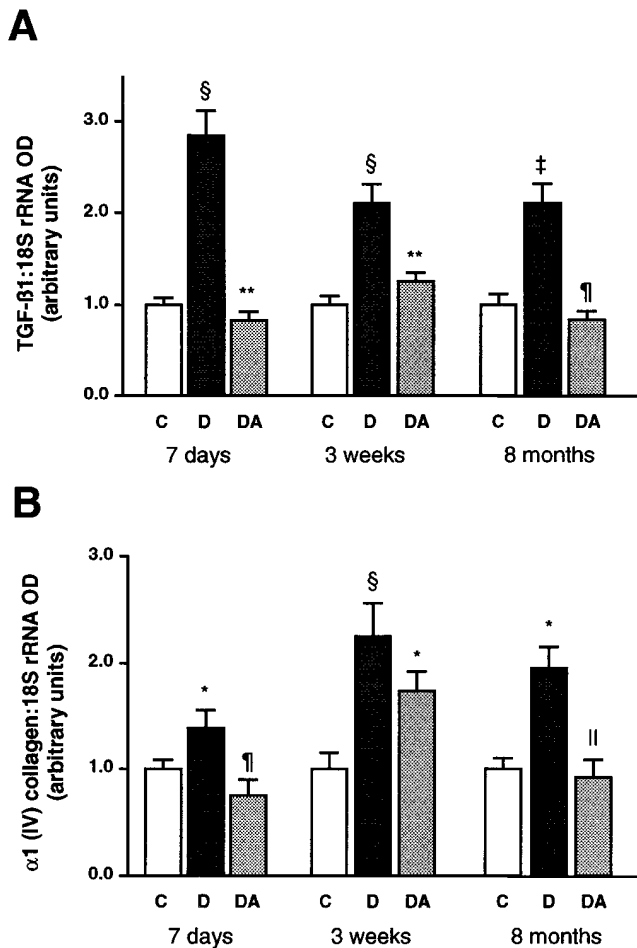
A

B

Figure 3. Quantitation of mesenteric TGF-β1 (*A*) and α1 (IV) collagen (*B*) mRNA. Data are shown as mean±SE of the ratio of optical density (OD) of specific mRNA to that of 18S rRNA, relative to control animals (designated an arbitrary value of 1) at 7 d, 3 wk, and 8 mo. $*P < 0.05$, $^{\ddagger}P < 0.01$, $^{\S}P < 0.001$ vs. C; $^{\parallel}P < 0.05$, $^{\P}P < 0.01$, $**P < 0.001$ vs. D. C, control; D, diabetic; A, aminoguanidine.

teric vessels compared with controls (Fig. 9). This was attenuated by AG treatment to levels observed in control rats.

AGE staining. The presence of AGEs was demonstrated immunohistochemically in the mesenteric vessels of diabetic animals (Fig. 10). By semiquantitative scoring more AGE was observed in tissue from diabetic compared with control rats (control, 1.3±0.2; diabetic, 2.8±0.2; $P < 0.001$). AG treatment significantly reduced the extent of AGE staining in diabetic vessels to levels observed in control rats (1.3±0.2; $P < 0.001$ vs. diabetic).

AGE radioimmunoassay. AGE content was significantly increased in the mesenteric vessels of diabetic animals compared to controls (control, 85±4; diabetic, 98±2 ng AGE/μg protein; $P < 0.01$). AG treatment significantly reduced detected AGEs in diabetic vessels to levels similar to those observed in control rats (83±2 ng AGE/μg protein; $P < 0.001$ vs. diabetic).

Discussion

The present study demonstrates that vascular hypertrophy in experimental diabetes is associated with increased TGF-β1
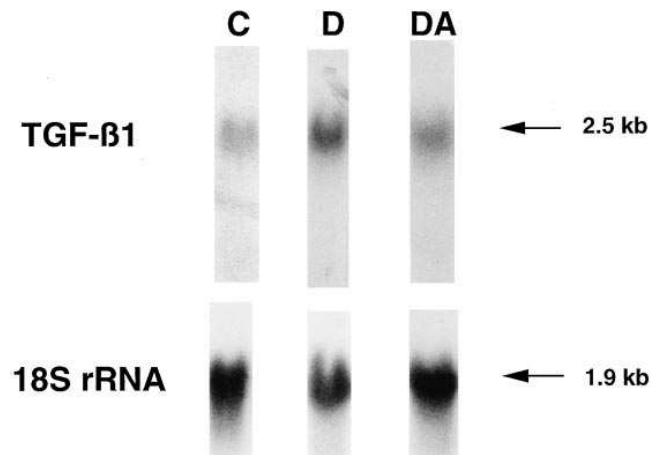

Figure 4. Northern blot of mesenteric vessel mRNA for TGF-β1 in control (C), diabetic (D), and diabetic + aminoguanidine (DA) rats. Increased gene expression of TGF-β1 at 7 d is seen with diabetes and is reduced by aminoguanidine.

mRNA and that this overexpression, in conjunction with increased vessel weight and ECM expansion, was attenuated by treatment with aminoguanidine. These findings implicate AGE formation in TGF-β overexpression and changes in tissue structure in diabetes.

Experimental evidence suggests that vascular hypertrophy may be an important process underlying the development of microvascular complications in diabetes. After the induction of experimental diabetes the glomerular capillary tuft undergoes hypertrophy accompanied by increased blood flow (35). These early changes are believed to be pathogenetically linked to the subsequent development of expansion of mesangial ECM and increased permeability to macromolecules (36, 37). Similar vascular enlargement occurs in mesenteric vessels in diabetes (7–9) which, like the glomerulus, is subject to hyperperfusion (17). Indeed, diabetes associated vascular changes with alterations in ECM and permeability is a widespread phenomenon with changes reported in the aorta (38), coronary arteries (39), and muscle capillaries (1) in addition to the mesentery and kidney.

The mesenteric vascular hypertrophy that accompanies diabetes may reflect diabetes-induced hyperphagia. However, previous studies in our laboratory have shown that angiotensin converting enzyme (ACE) inhibition can attenuate mesenteric vascular hypertrophy without reducing the increased food intake in diabetic rats (8). Similarly, in the present study AG prevented mesenteric vascular hypertrophy, without influencing food intake or glycemic control. The capacity of AG to decrease vessel hypertrophy during experimental diabetes suggests a trophic effect of AGEs and the inhibition of this action by AG.

While insulin has anabolic, growth-promoting actions, previous studies by our group have shown that insulin per se does not affect mesenteric vascular hypertrophy (8). However, normalization of plasma glucose in STZ-diabetic rats by insulin implants is associated with attenuation of vascular hypertrophy (8). These findings suggest a glucose-dependent mechanism, such as advanced glycation, in the pathogenesis of mesenteric vascular hypertrophy in diabetes.

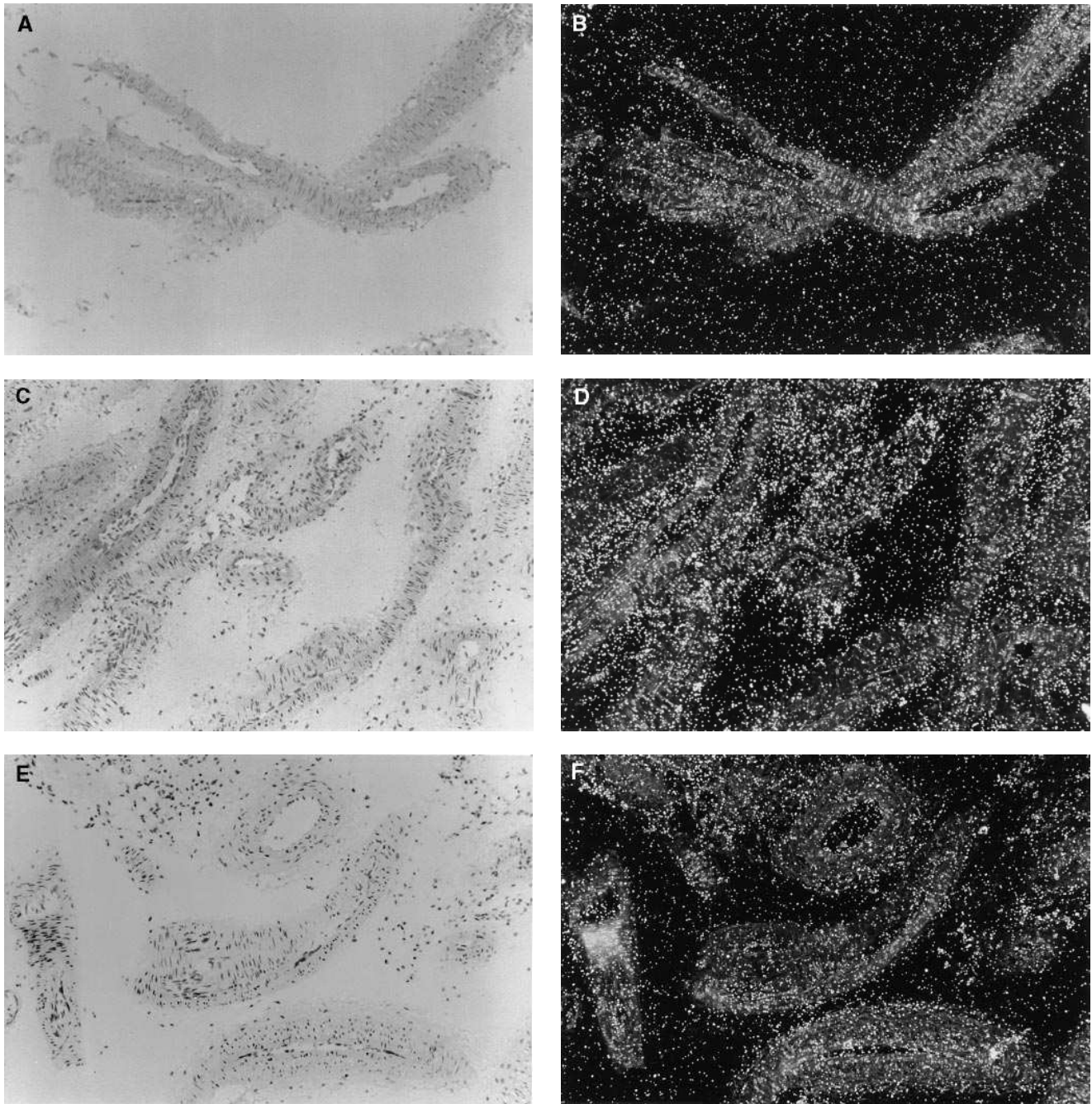Several significant abnormalities in liver function were ob-

Figure 5. Representative lightfield and darkfield photomicrographs of mesenteric arteries from 7 d control (*A*, *B*), diabetic (*C*, *D*), and AG treated diabetic rats (*E*, *F*) labeled in situ with a radiolabeled TGF-β1 riboprobe (×140).

served in diabetic rats. A low serum albumin was observed in the diabetic rats as has been previously noted by our group (40). Diabetic rats had an increase in serum alkaline phosphatase, of probable hepatic origin, as previously reported (41). Importantly, none of these parameters were influenced by AG treatment, except for a modest increase in the enzyme ALT. These findings warrant confirmation and further investigation.

A recent preliminary report has suggested that AGEs are present in food and that their clearance may be impaired in diabetes (42). However, although food intake is increased in diabetic rats, this hyperphagia was not attenuated by AG which

nevertheless prevented mesenteric vascular hypertrophy. Furthermore, AG acts predominantly by inhibiting the formation of AGEs and thus would not be expected to exert a beneficial action on preformed AGEs. However, such an effect cannot be excluded because concomitant administration of advanced glycated albumin and AG has been reported to decrease renal and systemic AGE accumulation (16).

Several studies in both experimental animals and man implicate overproduction of TGF-β in the pathogenesis of diabetic glomerulosclerosis (43, 44). Similarly, the results of the present study support the role of this prosclerotic cytokine in the pathogenesis of ECM expansion in the mesenteric vascular
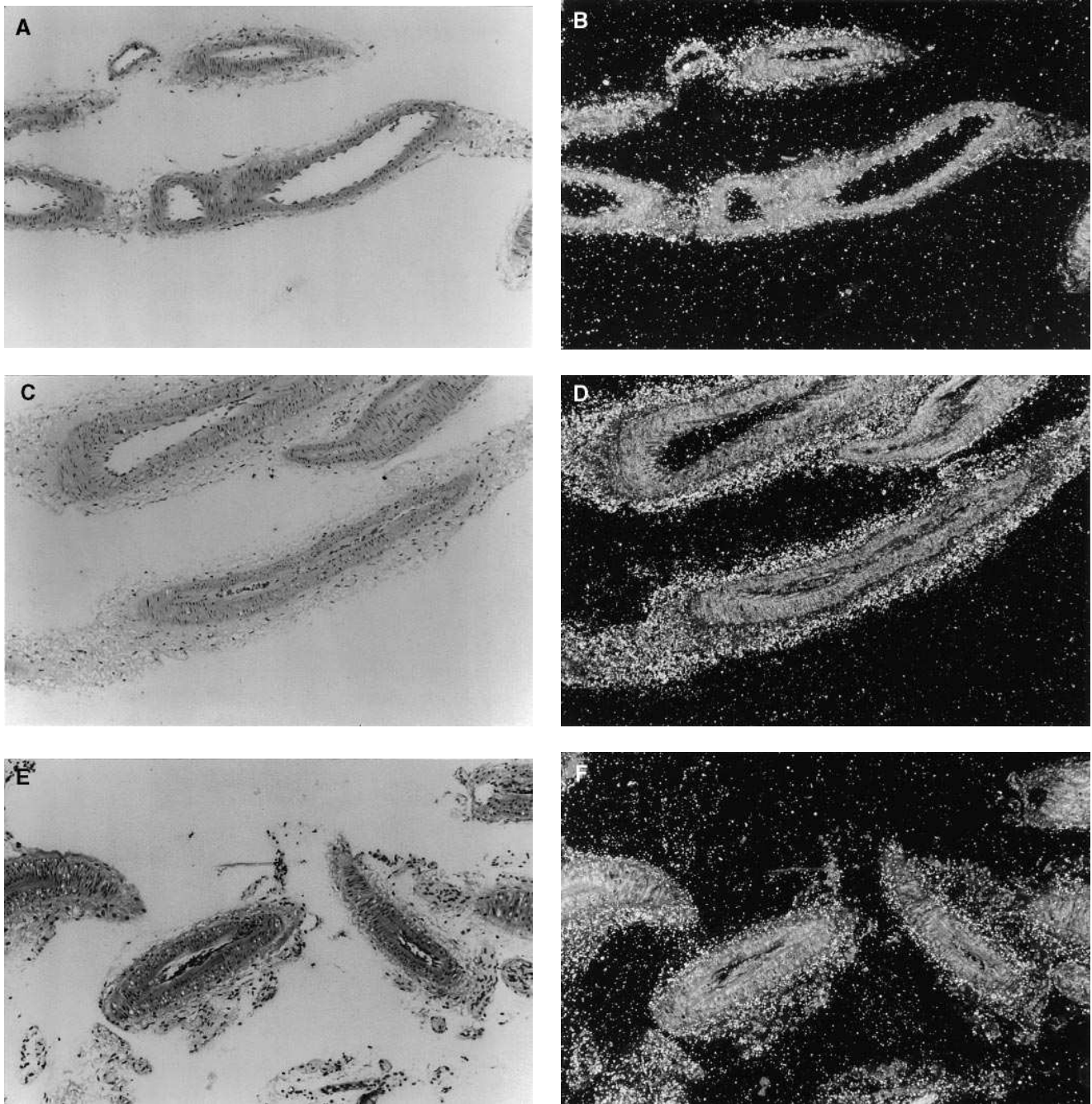
Figure 6. Representative lightfield and darkfield photomicrographs of mesenteric arteries from 7 d control (*A*, *B*), diabetic (*C*, *D*) and AG treated diabetic rats (*E*, *F*) labeled in situ with a radiolabeled βig-h3 riboprobe (×140).

bed in diabetes. TGF-β influences ECM in several ways including increased ECM synthesis, decreased ECM degradation, and modulation of the interaction between ECM and neighboring cells (14). However, the effects of TGF-β on cell proliferation are more complex with growth inhibitory and stimulatory actions both reported in vitro (45, 12). In vivo, neutralizing anti–TGF-β antibodies suppress intimal hyperplasia after rat carotid artery injury (13) and diabetes-related kidney growth (46). In addition, myoblasts stably transfected to overexpress TGF-β in an intracardiac graft promoted vascular endothelial cell DNA synthesis (47). These findings suggest that, in addition to its ability to stimulate ECM accumulation,

TGF-β may also contribute to the cell proliferation found in diabetes associated mesenteric vascular hypertrophy (48).

In situ studies revealed only sparse hybridization for TGF-β1 in control animals. In contrast, diabetes was associated with TGF-β mRNA in both the adventitia and intima. The expression of TGF-β1 transcripts by intimal cells may reflect a nonspecific response with similar changes reported after balloon catheter injury (49). However, in contrast to the expression of TGF-β by vascular smooth muscle cells in culture (50), the present study did not find TGF-β1 expression in the mesenteric arterial media, possibly reflecting phenotypic changes with in vitro passage.
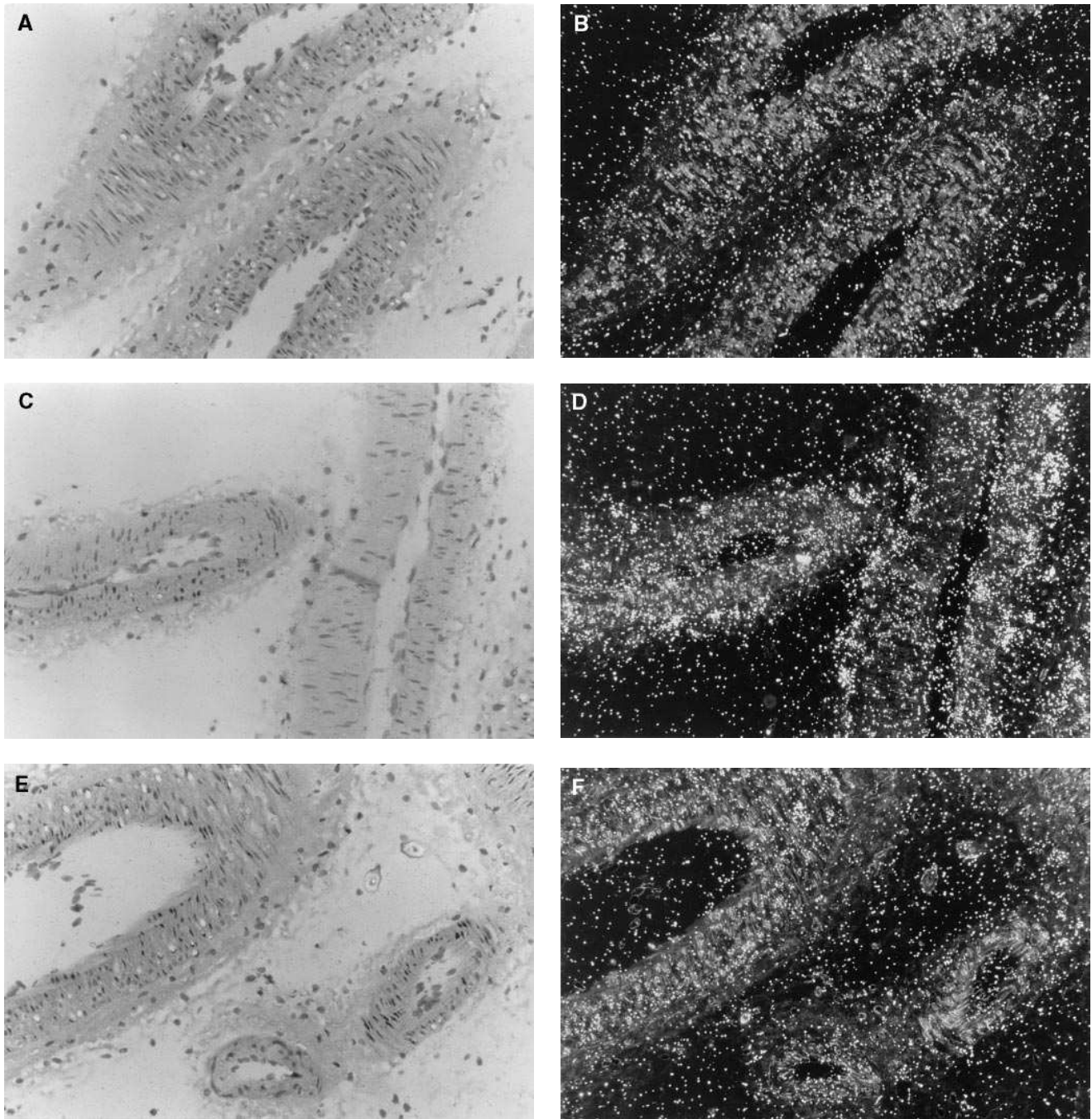
Figure 7. Representative lightfield and darkfield photomicrographs of mesenteric arteries from 7 d control (*A*, *B*), diabetic (*C*, *D*), and AG treated diabetic rats (*E*, *F*) labeled in situ with a radiolabeled α1 (IV) collagen riboprobe (×280).

TGF-β is bound to a latency-associated peptide such that gene expression or protein content may not necessarily reflect TGF-β biological activity. Methodological approaches to overcome this problem include the mink lung epithelium bioassay (51), measurement of specific fibronectin transcripts (52), or quantitating the expression of a TGF-β inducible gene such as βig-h3 (22). The latter is a recently identified secreted protein, the expression of which is highly responsive to TGF-β1 and which has been recently found to be present in vascular tissue (32). In the present study gene expression of βig-h3 paralleled that of TGF-β1 consistent with translation of TGF-β1 mRNA and subsequent secretion and activation.

The mechanisms responsible for the increased TGF-β1 mRNA levels observed in diabetic mesenteric arteries in the present study may be multiple. High glucose induces TGF-β expression in vitro in many cell lines, although the precise mechanisms which lead to this altered gene regulation are not well understood. Proposed mechanisms which may give rise to the TGF-β1 overexpression in the present study include glucose mediated activation of protein kinase C (53), cell stretch associated with the hyperperfusion (54), the production of Amadori-glycated proteins (55), and AGEs (16).

AGEs are produced from a complex interaction between non-enzymatically glycated proteins that form as a conse-
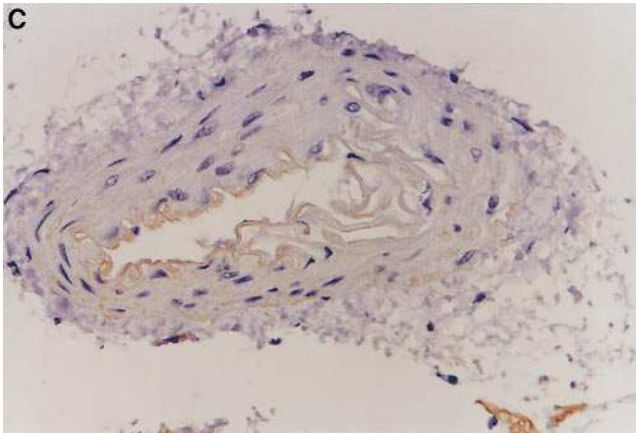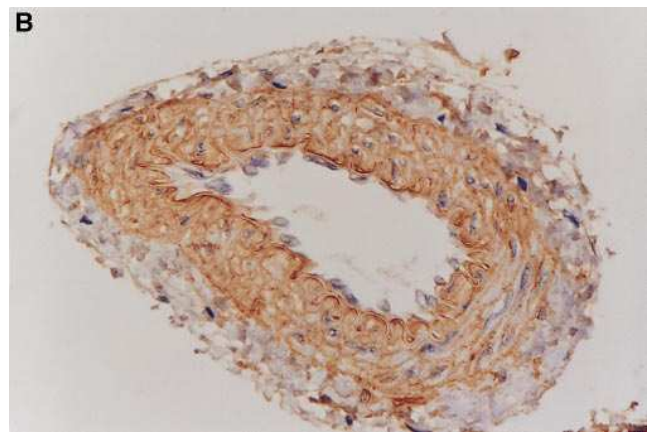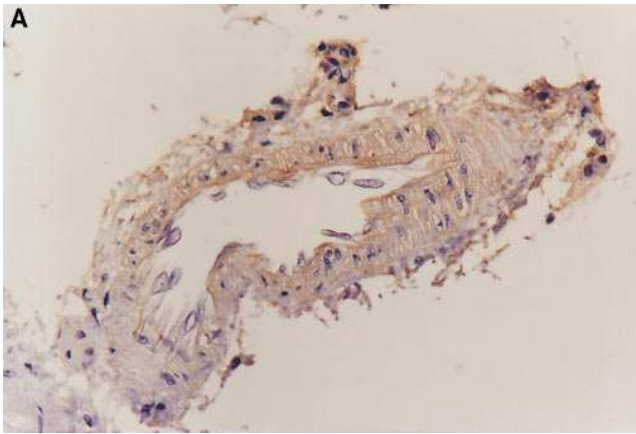
Figure 8. Representative light micrographs of mesenteric vessels in 7 d control (*A*), diabetic (*B*), and diabetic + aminoguanidine (*C*) rats. Type IV collagen in media stained with antibody to $\alpha 1$ (IV) collagen ($\times 550$).
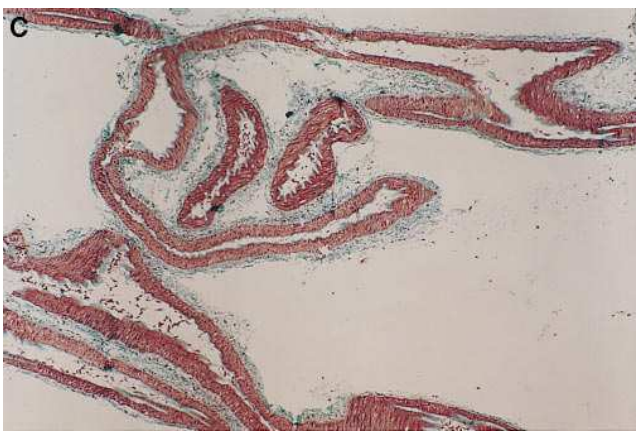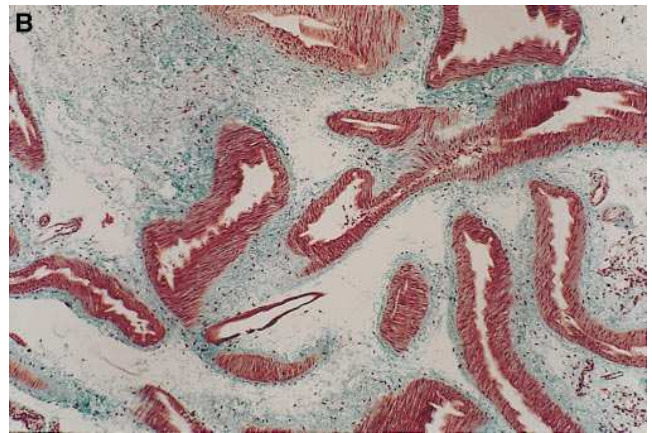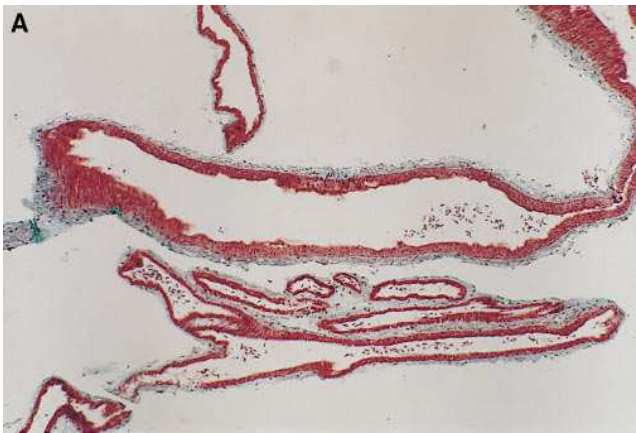

Figure 9. Representative light micrographs of mesenteric vessels in 3 wk control (*A*), diabetic (*B*), and diabetic + aminoguanidine (*C*) rats. Collagen stained with a trichrome stain ($\times 140$).
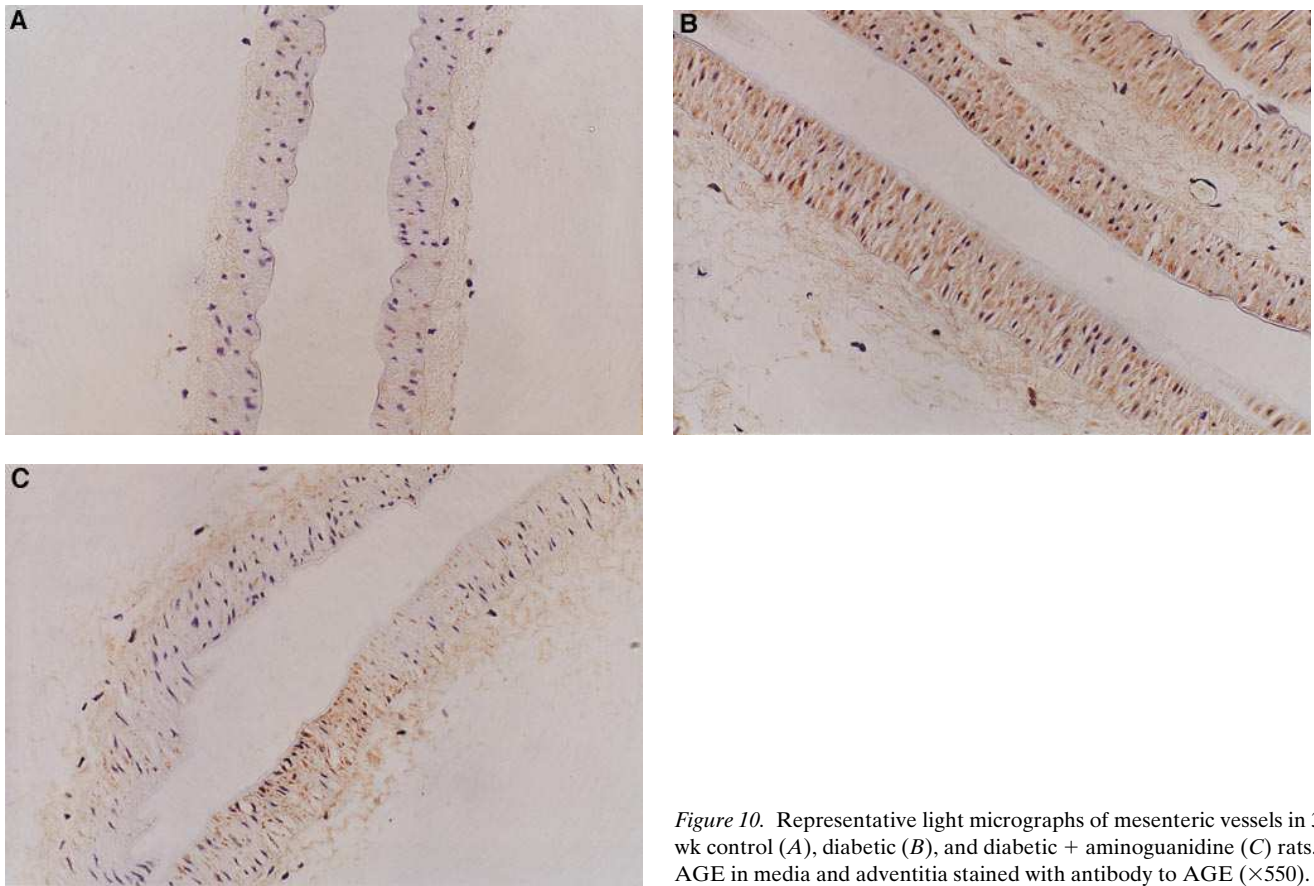
Figure 10. Representative light micrographs of mesenteric vessels in 3 wk control (*A*), diabetic (*B*), and diabetic + aminoguanidine (*C*) rats. AGE in media and adventitia stained with antibody to AGE (×550).

quence of the Maillard reaction (31). This process is accelerated in diabetes presumably as a consequence of the increased glucose concentration in the extracellular fluid. AGEs accumulate in blood vessels, and often tissues, and are believed to contribute to degenerative changes that characterize the aging process. For instance, in the vessel wall AGEs are associated with sequestration of low density lipoproteins as well as causing increased vascular permeability (56). Other sequelae of accumulated vascular AGEs include vessel wall stiffness with impairment of myogenic reactivity (57), vascular permeability and impaired vasodilatory responses (58, 59). These changes may be ameliorated by reducing AGE formation by AG with resulting increased vessel elasticity (60) and reduced sclerosis (16).

In the present study AGEs were identified by immunohistochemical analysis and RIA in mesenteric vessels within 3 wk after the induction of experimental diabetes. Furthermore, the accumulation of AGEs at this site was prevented by AG administration. The early appearance of AGEs in our study is consistent with the findings of other groups which have demonstrated the accumulation of AGEs in skeletal muscle arterioles within 4–6 wk of experimental diabetes (57).

The concept that AGEs exert effects through receptor-dependent mechanisms has been substantiated by the identification of specific receptors (61, 62). In vivo studies have shown that administration of AGE-modified mouse serum albumin, generated in vitro, induced gene expression of $\alpha 1$ (IV) collagen and transforming growth factor-β1 in glomeruli (16). Moreover, AGEs have been shown to interact with vascular endothelium by receptor mediated mechanisms which lead to induction of interleukin-6 mRNA (63). The present study sought

to examine the contribution of AGE formation in vivo to TGF-β1 overexpression and vascular hypertrophy in diabetes by inhibiting their formation with AG. The findings that AG treatment ameliorated vascular hypertrophy, ECM expansion, and TGF-β1 overexpression in diabetic animals without affecting blood glucose levels provide evidence that in vivo AGE formation may contribute to the pathogenesis of tissue remodeling in diabetes. Furthermore, the findings in the present study suggest that AGEs may mediate at least some of their pathogenetic effects by induction of TGF-β transcription. This is consistent with results of studies in experimental diabetes which demonstrate the ability of AG to reduce mesangial ECM expansion (3), an aspect of diabetic kidney disease in which TGF-β has been consistently implicated (43).

Although the principal mechanism of action of AG is inhibition of the formation of AGEs, it may also inhibit nitric oxide (NO) production (64, 65). This action of AG is potentially relevant to the complications of diabetes as NO, an endothelial cell product, is a potent vasodilator. Although in certain vascular trees in experimental diabetes there is evidence of increased NO production (66), mesenteric vascular hypertrophy is not attenuated by specific NO inhibition with L-nitro-arginine-methyl-ester (9) suggesting that the demonstrated effect of AG in the present study was not mediated by an effect on NO synthesis.

While AG therapy may lead to a reduction in TGF-β expression, this does not imply that AGE formation is the sole pathogenetic mechanism in tissue remodeling and ECM accumulation in diabetes. For instance, angiotensin converting enzyme inhibition has also been shown to reduce glomerular hy-

pertrophy and albuminuria in diabetic rats (67, 68). Furthermore, such treatment also reduces mesenteric vascular growth in experimental diabetes (7–9). However, while angiotensin II may increase TGF-β mRNA in vitro (52) this has not been confirmed in vivo as treatment of diabetic rats with the angiotensin converting enzyme inhibitor enalapril did not reduce glomerular TGF-β overexpression in diabetic rats (69) despite reducing ECM gene expression (70).

While AGEs are traditionally believed to develop slowly, other recent studies suggest that their effects may be manifest early in experimental diabetes (57, 58). This is consistent with a possible role for AGEs in changes associated with tissue senescence. For instance, AG has been shown to attenuate age-related changes such as glomerular obsolescence and cardiac hypertrophy in nondiabetic rats (71). Furthermore, AG has been considered to have a potential protective role in atherosclerosis where it has been shown to decrease plaque formation in the cholesterol fed nondiabetic rabbit (72), possibly reflecting a reduction in the augmented TGF-β production found in this condition.

The present study suggests that AGEs may play a role in the increased TGF-β1 expression and vascular changes observed in experimental diabetes. The ability of aminoguanidine to ameliorate these changes provides a pathogenetic basis for the potential use of this agent in the prevention of the long-term vascular complications of diabetes.

Acknowledgments

References

1. Williamson, J.R., R.G. Tilton, K. Chang, and C. Kilo. 1988. Basement membrane abnormalities in diabetes mellitus: relationship to clinical microangiopathy. *Diabetes Metab. Rev.* 4:339–370.

2. Brownlee, M.A., A. Cerami, and H. Vlassara. 1988. Advanced glycosylation end products in tissue and the biochemical basis of diabetic complications. *N. Engl. J. Med.* 318:131–138.

3. Soulis-Liparota, T., M. Cooper, D. Papazoglou, B. Clarke, and G. Jerums. 1991. Retardation by aminoguanidine of development of albuminuria, mesangial expansion, and tissue fluorescence in streptozocin-induced diabetic rat. *Diabetes.* 40:1328–1334.

4. Hammes, H-P., D. Strodter, A. Weiss, R.G. Bretzel, K. Federlin, and M. Brownlee. 1995. Secondary intervention with aminoguanidine retards the progression of diabetic retinopathy in the rat model. *Diabetologia.* 38:656–660.

5. Griffin, S.A., W.C. Brown, F. MacPherson, J.C. McGrath, V.G. Wilson, N. Korsgaard, M.J. Mulvany, and A.F. Lever. 1991. Angiotensin II causes vascular hypertrophy in part by a non-pressor mechanism. *Hypertension.* 17:626–635.

6. Simonsen, U., E. Ehrnrooth, L.U. Gerdes, O. Faergemann, J. Buch, F. Andreasen, and M.J. Mulvany. 1991. Functional properties in vitro of systematic small arteries from rabbits fed a cholesterol-rich diet for 12 weeks. *Clin. Sci. (Lond.).* 80:119–129.

7. Vranes, D., M.E. Cooper, and R.J. Dilley. 1995. Angiotensin converting enzyme inhibition reduces diabetes-induced vascular hypertrophy: Morphometric analysis. *J. Vasc. Res.* 32:183–189.

8. Cooper, M.E., J. Rumble, R. Komers, H-C. Du, K. Jandeleit, and S.T. Chou. 1994. Diabetes-associated mesenteric vascular hypertrophy is attenuated by angiotensin converting enzyme inhibition. *Diabetes.* 43:1221–1228.

9. Rumble, J.R., R. Komers, and M.E. Cooper. 1996. Kinins/nitric oxide are involved in the antihypertrophic effect of ACE inhibitors on diabetes-associated mesenteric vascular hypertrophy in the rat. *J. Hypertens.* 14:601–607.

10. Sarzani, R., P. Brecher, and A.V. Chobanian. 1989. Growth factor expression in aorta of normotensive and hypertensive rats. *J. Clin. Invest.* 83: 1404–1408.

11. Yamamoto, T., T. Nakamura, N.A. Noble, E. Ruoslahti, and W.A. Border. 1993. Expression of transforming growth factor beta is elevated in human and experimental diabetic nephropathy. *Proc. Natl. Acad. Sci. USA.* 90:1814–1818.

12. Stouffer, G.A., and G.K. Owens. 1994. TGF-β promotes proliferation of cultured SMC via both PDGF-AA-dependent and PDGF-AA-independent mechanisms. *J. Clin. Invest.* 93:2048–2055.

13. Wolf, Y.G., L.M. Rasmussen, and E. Ruoslahti. 1994. Antibodies against transforming growth factor-β suppress intimal hyperplasia in a rat model. *J. Clin. Invest.* 93: 1172–1178.

14. Border, W.A., and N.A. Noble. 1994. Mechanisms of disease: Transforming growth factor-β in tissue fibrosis. *N. Engl. J. Med.* 331:1286–1292.

15. Throckmorton, D.C., A.P. Brogden, B. Min, H. Rasmussen, and M. Kashgarian. 1995. PDGF and TGF-β mediate collagen production by mesangial cells exposed to advanced glycosylation end products. *Kidney Int.* 48:111–117.

16. Yang, C.W., H. Vlassara, E.P. Peten, C.J. He, G.E. Striker, and L.J. Striker. 1994. Advanced glycation end products up-regulate gene expression found in diabetic glomerular disease. *Proc. Natl. Acad. Sci. USA.* 91:9436–9440.

17. Kiff, R.J., S.M. Gardiner, A.M. Compton, and T. Bennett. 1991. The effects of endothelin-1 and NG-nitro-L-arginine methyl ester on regional haemodynamics in conscious rats with streptozotocin-induced diabetes mellitus. *Br. J. Pharmacol.* 103:1321–1326.

18. Bunag, R.D. 1973. Validation in awake rats of a tail-cuff method for measuring systolic pressure. *J. Appl. Physiol.* 34:279–282.

19. Schmidt, F.H. 1961. Enzymatic determination of glucose and fructose simultaneously. *Klin. Wochenschr.* 39:1244–1247.

20. Allen, T.J., M.E. Cooper, R.C. O'Brien, L.A. Bach, B. Jackson, and G. Jerums. 1990. Glomerular filtration rate in the streptozocin diabetic rat: The role of exchangeable sodium, vasoactive hormones and insulin therapy. *Diabetes.* 38:1182–1190.

21. Chomczynski, P., and N. Sacchi. 1987. Single step method of RNA isolation by acid guanidinium thiocyanate-phenol-chloroform extraction. *Anal. Biochem.* 162:156–159.

22. Skonier, J., K. Bennett, V. Rothwell, S. Kosowski, G. Plowman, P. Wallace, S. Edelhoff, C. Disteche, M. Neubauer, H. Marquardt, J. Rodgers, et al. 1994. Beta ig-h3: a transforming growth factor beta responsive gene encoding a secreted protein that inhibits cell attachment in vitro and suppresses the growth of CHO cells in nude mice. *DNA Cell Biol.* 13:571–574.

23. Duncan, M.K., T. Shimamura, and K. Chada. 1994. Expression of the helix-loop-helix protein, ID, during branching morphogenesis in the kidney. *Kidney Int.* 46:324–332.

24. Gilbert, R.E., P.G. McNally, A. Cox, M. Dziadek, J.R. Rumble, M.E. Cooper, and G. Jerums. 1995. Gene expression of the anti-adhesive extracellular matrix protein secreted protein acidic and rich in cysteine (SPARC) is reduced in early diabetes related kidney growth. *Kidney Int.* 48:1216–1225.

25. Elias, J.M. 1990. Immunohistopathology: A Practical Approach to Diagnosis. ASCP Press, Chicago. 21–29.

26. Kranzfofer, R., J. Schirmer, A. Schomig, E. von Hodenberg, E. Pestel, J. Metz, H.J. Lang, and W. Kubler. 1993. Suppression of neointimal thickening and smooth muscle cell proliferation after arterial injury in the rat by inhibitors of Na(+)-H+ exchange. *Circ. Res.* 73(2):264–268.

27. Kakinuma, Y., T. Kawamura, T. Bills, T. Yoshiola, I. Ichikawa, and A. Fogo. 1992. Blood pressure independent effect of angiotensin inhibition on vascular lesions in chronic renal failure. *Kidney Int.* 42:46–55.

28. Floege, J., C.E. Alpers, M.W. Burns, P. Pritzl, K. Gordon, W.G. Couser, and R.J. Johnson. 1992. Glomerular cells, extracellular matrix accumulation, and the development of glomerulosclerosis in the remnant kidney model. *Lab. Invest.* 66:485–497.

29. Gugliucci, A., and M. Bendayan. 1996. Renal fate of circulating advanced glycated end products (AGE): evidence for reabsorption and catabolism of AGE-peptides by renal proximal tubular cells. *Diabetologia.* 39:149–160.

30. Soulis, T., M.E. Cooper, D. Vranes, R. Bucala, and G. Jerums. 1996. The effects of aminoguanidine in preventing experimental diabetic nephropathy are related to the duration of treatment. *Kidney Int.* 50:627–634.

31. Monnier, V.M., V.J. Stevens, and A. Cerami. 1981. Maillard reactions involving proteins and carbohydrates in vivo: Relevance to diabetes mellitus and aging. *Prog. Food Nutr. Sci.* 5:315–327.

32. O'Brien, E.R., K.L. Bennett, M.R. Garvin, T.W. Zderic, T. Hinohara, J.B. Simpson, T. Kimura, M. Nobuyoshi, A. Purchio, et al. 1996. Beta ig-h3, transforming growth factor-beta-inducible gene, is overexpressed in atherosclerotic and restenotic human vascular lesions. *Arterioscler. Thromb. Vasc. Biol.* 16:576–584.

33. Masson, P. 1929. Trichrome stainings and their preliminary technique. *J. Tech. Methods.* 2:75–90.

34. Snedecor, G.W., and W.G. Cochran. 1980. Statistical Methods. 7th ed. Iowa State University Press, Ames, Iowa. 228–236.

35. Brenner, B.M. 1983. Hemodynamically mediated glomerular injury and the progressive nature of kidney disease. *Kidney Int.* 23:647–655.

36. Seyer-Hansen, K. 1983. Renal hypertrophy in experimental diabetes mellitus. *Kidney Int.* 23:643–646.

37. Rasch, R. 1980. Prevention of diabetic glomerulopathy in streptozotocin diabetic rats by insulin treatment; albumin excretion. *Diabetologia.* 18:413–416.

38. Wasty, F., M.Z. Alavi, and S. Moore. 1993. Distribution of glycosaminoglycans in the intima of human aortas: changes in atherosclerosis and diabetes. *Diabetologia.* 36:316–322.

39. Dybdahl, H., and T. Ledet. 1987. Diabetic macroangiopathy. Quantitative histopathological studies of the extramural coronary arteries from type 2 (non-insulin-dependent) diabetic patients. *Diabetologia.* 30:882–886.

40. Hulthen, U.L., Z. Cao, J.R. Rumble, M.E. Cooper, and C.I. Johnston. 1996. Vascular hypertrophy and albumin permeability in a rat model combining hypertension and diabetes mellitus. Effects of calcium antagonism, angiotensin converting enzyme inhibition and angiotensin II AT-1 receptor blockade. *Am. J. Hypertens.* 9:895–901.

41. Gonzalez, J., and J. Fevery. 1992. Spontaneously diabetic biobreeding rats and impairment of bile acid-independent bile flow and increased biliary bilirubin, calcium and lipid secretion. *Hepatology.* 16:426–432.

42. Koschinsky, T., C. He, T. Mitsuhashi, C. Liu, C. Buenting, K. Heitmann, and H. Vlassara. 1996. Impaired clearance of toxic food-derived advanced glycation endproducts as a risk for diabetic nephropathy. *Diabetologia.* 39:(Suppl 1):A70 (Abstr).

43. Ziyadeh, F.N., and K. Sharma. 1995. Role of transforming growth factor-β in diabetic glomerulosclerosis and renal hypertrophy. *Kidney Int.* 48:S34–S36.

44. Yokoyama, H., and T. Deckert. 1996. Central role of TGF-β in the pathogenesis of diabetic nephropathy and macrovascular complications: a hypothesis. *Diabetic Med.* 13:313–320.

45. MacKay, K., L.J. Striker, J.W. Stauffer, T. Doi, L.Y. Agoda, and G.E. Striker. 1989. Transforming growth factor-β. Murine glomerular receptors and responses of isolated glomerular cells. *J. Clin. Invest.* 83:1160–1167.

46. Sharma, K., Y. Jin, J. Guo, and F.N. Ziyadeh. 1996. Neutralization of TGF-beta by anti-TGF-beta antibody attenuates kidney hypertrophy and the enhanced extracellular matrix gene expression in STZ-induced diabetic mice. *Diabetes.* 45:522–530.

47. Koh, G.Y., S.-J. Kim, M.G. Klug, K. Park, M.H. Soonpaa, and L.J. Field. 1995. Targeted expression of transforming growth factor-β1 in intracardiac grafts promotes vascular endothelial cell DNA synthesis. *J. Clin. Invest.* 95:114–121.

48. Vranes, D., R.J. Dilley, and M.E. Cooper. 1995. Diabetes associated vascular hypertrophy is associated with endothelial proliferation. *Diabetologia.* 38(Suppl 1):A255 (Abstr).

49. Wysocki, S.J., M.-H. Zheng, Y. Fan, M.D. Lamawansa, A.K. House, and P.E. Norman. 1996. Expression of transforming growth factor-β1 (TGF-β1) and urokinase-type plasminogen activator (u-PA) genes during arterial repair in the pig. *Cardiovasc. Res.* 31:28–36.

50. Gibbons, G.H., R.E. Pratt, and V.J. Dzau. 1992. Vascular smooth muscle cell hypertrophy vs. hyperplasia. *J. Clin. Invest.* 90:456–461.

51. Ralph, D., M. McClelland, and J. Welsh. 1993. RNA fingerprinting using arbitrarily primed PCR identifies differentially regulated RNAs in mink lung (Mv1Lu) cells growth arrested by transforming growth factor beta 1. *Proc. Natl. Acad. Sci. USA.* 90:10710–10714.

52. Kagami, S., W.A. Border, D.E. Miller, and N.A. Noble. 1994. Angiotensin II stimulates extracellular matrix protein synthesis through induction of transforming growth factor-β expression in rat glomerular mesangial cells. *J. Clin. Invest.* 93:2431–2437.

53. Kim, S.-J., F. Denhez, K.-Y. Kim, T.J. Holt, M.B. Sporn, and A.B. Roberts. 1989. Activation of the second promoter of the transforming growth factor-β1 gene and phorbol ester occurs through the same target sequences. *J. Biol. Chem.* 264:19373–19378.

54. Wilson, E., K. Sudhir, and H.E. Ives. 1995. Mechanical strain of rat vascular smooth muscle cells is sensed by specific extracellular matrix/integrin interactions. *J. Clin. Invest.* 96:2364–2372.

55. Cohen, M.P., and F.N. Ziyadeh. 1996. Role of amadori-modified nonenzymatically glycated serum proteins in the pathogenesis of diabetic nephropathy. *J. Am. Soc. Nephrol.* 7:183–190.

56. Brownlee, M., H. Vlassara, and A. Cerami. 1985. Non-enzymatic glycosylation products on collagen covalently trap low-density lipoprotein. *Diabetes.* 34:938–941.

57. Hill, M.A., and E.A. Ege. 1994. Active and passive mechanical properties of isolated arterioles from STZ-induced diabetic rats: effect of aminoguanidine treatment. *Diabetes.* 43:1450–1456.

58. Bucala, R., K.J. Tracey, and A. Cerami. 1991. Advanced glycosylation products quench nitric oxide and mediate defective endothelium-dependent vasodilatation in experimental diabetes. *J. Clin. Invest.* 87:432–438.

59. Vlassara, H., H. Fuh, Z. Makita, S. Krungkrai, A. Cerami, and R. Bucala. 1992. Exogenous advanced glycation end products induce complex vascular dysfunction in normal animals. *Proc. Natl. Acad. Sci. USA.* 89:12043–12047.

60. Huijberts, M.S.P., B.H.R. Wolffenbuttel, H.A.J. Struijker Boudier, F.R.L. Crijns, A.C. Nieuwenhuijzen Kruseman, P. Poitevin, and B.I. Levy. 1993. Aminoguanidine treatment increases elasticity and decreases fluid filtration of large arteries from diabetic rats. *J. Clin. Invest.* 92:1407–1411.

61. Schmidt, A.M., M. Vianna, M. Gerlach, J. Brett, J. Ryan, J. Kao, C. Esposito, H. Hegarty, W. Hurley, M. Clauss, et al. 1992. Isolation and characterisation of two binding proteins for advanced glycation end products from bovine lung which are present on the endothelial cell surface. *J. Biol. Chem.* 267:14987–14997.

62. Vlassara, H. 1995. Receptors for advanced glycation endproducts: In vivo role and human studies. *In* Diabetes 1994. S. Baba and T. Kaneko, editors. Elsevier Science Publishing Co. Inc., New York. 286–291.

63. Schmidt, A.M., M. Hasu, D. Popov, J.H. Zhang, J. Chen, S.D. Yan, J. Brett, R. Cao, K. Kuwabara, G. Costache, et al. 1994. Receptor for advanced glycation end products (AGEs) has a central role in vessel wall interactions and gene activation in response to circulating AGE proteins. *Proc. Natl. Acad. Sci. USA.* 91:8807–8811.

64. Corbett, J.A., R.G. Tilton, K. Chang, K.S. Hasan, Y. Ido, J.L. Wang, M.A. Sweetland, J.R. Lancaster Jr., J.R. Williamson, and M.L. McDaniel. 1992. Aminoguanidine, a novel inhibitor of nitric oxide formation, prevents diabetic vascular dysfunction. *Diabetes.* 41:552–556.

65. Tilton, R.G., K. Chang, K.S. Hasan, S.R. Smith, J.M. Petrash, T.P. Misko, W.M. Moore, M.G. Currie, J.A. Corbett, M.L. McDaniel, et al. 1993. Prevention of diabetic vascular dysfunction by guanidines: Inhibition of nitric oxide synthase versus advanced glycation end-product formation. *Diabetes.* 42:221–232.

66. Komers, R., T.J. Allen, and M.E. Cooper. 1994. Role of endothelium-derived nitric oxide in the pathogenesis of the renal hemodynamic changes of experimental diabetes. *Diabetes.* 43:1190–1197.

67. Cooper, M.E., T.J. Allen, R.C. O'Brien, D. Papazoglou, B. Clarke, G. Jerums, and A.E. Doyle. 1990. Nephropathy in a model combining genetic hypertension with experimental diabetes: Enalapril versus hydralazine and metoprolol therapy. *Diabetes.* 39:1575–1579.

68. Rumble, J.R., A.E. Doyle, and M.E. Cooper. 1995. Comparison of effects of ACE inhibition with calcium channel blockade on renal disease in a model combining genetic hypertension with diabetes. *Am. J. Hypertens.* 8:53–57.

69. Fukui, M., T. Nakamura, I Ebihara, Y. Makita, S. Osada, Y. Tomino, and H. Koide. 1994. Effects of enalapril on endothelin-1 and growth factor gene expression in diabetic rat glomeruli. *J. Lab. Clin. Med.* 123:763–768.

70. Nakamura, T., T. Takahashi, M. Fukui, I. Ebihara, S. Osada, Y. Tomino, and H. Koide. 1995. Enalapril attenuates increased gene expression of extracellular matrix components in diabetic rats. *J. Am. Soc. Nephrol.* 5:1492–1497.

71. Li, Y.M., Steffes, T. Donnelly, C. Liu, H. Fuh, J. Basgen, R. Bucala, and H. Vlassara. 1996. Prevention of cardiovascular and renal pathology of aging by the advanced glycation inhibitor aminoguanidine. *Proc. Natl. Acad. Sci. USA.* 93:3902–3907.

72. Jerums, G., T. Soulis, S. Panagiotopoulos, and M.E. Cooper. 1995. In vivo effects of aminoguanidine in experimental diabetes and atherosclerosis. *In* Diabetes 1994. S. Baba and T. Kaneko, editors. Elsevier Science Publishing Co. Inc., New York. 299–305.